JOURNAL OF MATERIALS SCIENCE 24 (1989) 541–548

Lead zinc niobate pyrochlore: structure and dielectric properties

H. C. LING
AT&T Bell Laboratories, Princeton, New Jersey 08540, USA
M. F. YAN, W. W. RHODES
AT&T Bell Laboratories, Murray Hill, New Jersey 07974, USA

In $Pb(B'_xB''_{1-x})O_3$ ceramic compositions, it is customary to find a mixture of cubic pyrochlore and perovskite phases after calcination. Based on X-ray diffraction analysis, we concluded that both phases are made up of the same structural unit of BO_6 octahedra. The B′ and B″ ions occupy the B sites randomly to the extent that local charge equilibrium is maintained. Thus a general formula for the pyrochlore phase can be expressed as $Pb(B'_xB''_{1-x})O_3 \cdot O_p$ where $0 \leqslant p \leqslant 0.5$. An extensive study of the $Pb(Zn_xNb_{1-x})O_{3.5-1.5x}$ pyrochlore system was made by varying the zinc concentration. We interpret changes in the X-ray diffraction pattern and the lattice constant as indicative of the changing occupancy of the seventh oxygen sites in order to maintain local charge balance. The best combination of the dielectric properties, with a dielectric constant of 130 and a Q factor greater than 1000 at 10 MHz, is achieved at a composition of $0.3 \leqslant x \leqslant 0.4$ and a sintering temperature of 980° C. The temperature coefficient of the dielectric constant measures $-0.75 \times 10^{-3}\,°C^{-1}$. It decreases to $-0.54 \times 10^{-3}\,°C^{-1}$ when 5 mol% of $PbTiO_3$ was mixed with the nominal pyrochlore compositions and sintered. Thus, it may be possible to effect a larger change in the temperature coefficient by judiciously including selective amounts of a second phase which has the best compensating temperature coefficient.

1. Introduction

The name pyrochlore originally referred to the mineral $NaCaNb_2O_6F$. Later, it was found [1] that compounds such as $Cd_2Nb_2O_7$, $Cd_2Ta_2O_7$, $Ca_2Ta_2O_7$ and $Pb_2Sb_2O_7$ all possess a similar cubic $E8_1$ structure to the pyrochlore. A great deal of interest was attracted to the pyrochlore structure when cadmium niobate was discovered to be ferroelectric [2, 3], with a Curie temperature of 185 K and a peak dielectric constant about 1200. However, the formation of solid solutions $Cd_2(Nb, Ta)_2O_7$ or $(Cd, Pb)Nb_2O_7$ invariably decreased the Curie temperature from that of pure $Cd_2Nb_2O_7$. Subsequent investigations of other systems did not reveal any new pyrochlore ferroelectrics.

In a study on the multiple cation substitution for the Ti^{4+} ion in the $PbTiO_3$ perovskite structure, we reported [4] that two crystalline phases, the perovskite and the pyrochlore, may co-exist in the temperature range between 800 and 1100° C. The perovskite structure is susceptible to the ferroelectric transition and exhibits a high dielectric constant (> 1000) at the Curie temperature. In contrast, the pyrochlore compounds are non-ferroelectric and have small dielectric constants (~ 100). In order to attain the maximum dielectric constant, the pyrochlore phase has to be eliminated completely. Otherwise, the dielectric constant will, to a first approximation, decrease proportionately with the volume fraction of the pyrochlore phase.

In this earlier study [4], we observed that in nominal compositions $Pb(B'_xB''_{1-x})^{4+}O_3$ where the B site has an average 4+ charge and B″ = Nb or Ta, the lattice constants of the pyrochlore and perovskite phases varied in a similar manner when the B′ cation was changed (see Fig. 1). Since the lattice parameter of the pyrochlore phase changes with the B′ cation, the pyrochlore cannot be represented by a simple chemical formula of $Pb_2Nb_2O_7$, which is rhombohedrally distorted at room temperature. Rather, the B′ cation must be inherently incorporated as part of the pyrochlore structure. Furthermore, the ratio of lattice parameters (a_{pyr}/a_{per}) is remarkably constant, with a maximum variation of 0.6% among all the compositions studied (Table I). Since the perovskite structure is quite well established with a chemical formula $Pb(B'_xB''_{1-x})O_3$, this strongly suggests that the structural unit in the pyrochlore phase is similar to that in the corresponding perovskite phase. Charge neutrality is maintained by the complete absence of the seventh set of oxygen atoms. Consequently, the chemical formula for the pyrochlore phase can be written as $Pb(B'_xB''_{1-x})^{4+}O_3 \cdot O_{p=0}$ or $Pb_2(B'_xB''_{1-x})_2O_6$.

If the average charge on the B site differs from 4+, one can anticipate a corresponding change in the number of oxygen atoms occupying the seventh (non-essential) sites. From the foregoing discussion, it would appear that the total number of oxygen atoms can vary between 3 and 3.5 without affecting the

0022–2461/89 $03.00 + .12 © *1989 Chapman and Hall Ltd.*

TABLE I Lattice constants of the pyrochlore and the perovskite phases in compositions $Pb(B'_xB''_{1-x})O_3$.*

Nominal composition	r (nm)	a (nm) Pyrochlore	Perovskite	$\frac{a_{per}}{a_{pyr}}$
$Pb(Mg_{1/3}Nb_{2/3})O_3$	0.065	1.0611	0.4047	2.6219
$Pb(Ni_{1/3}Nb_{2/3})O_3$	0.072	1.0591	0.4030	2.6280
$Pb(Zn_{1/3}Nb_{2/3})O_3$	0.074	1.0611	0.4040†	2.6265
$Pb(Fe_{1/3}Nb_{2/3})O_3$	0.076	1.0578	0.4014	2.6353
$Pb(Mn_{1/3}Nb_{2/3})O_3$	0.080	1.0589	0.4024	2.6315
$Pb(Mg_{1/3}Ta_{2/3})O_3$	0.065	1.0603	0.4040	2.6245
$Pb(Co_{1/3}Ta_{2/3})O_3$	0.074	1.0595	0.4040	2.6225
$Pb(Fe_{1/3}Ta_{2/3})O_3$	0.076	1.0559	0.4008	2.6345
$Pb(Mn_{1/3}Ta_{2/3})O_3$	0.080	1.0568	0.4024	2.6262
$Pb(Fe_{1/2}Ta_{1/2})O_3$	0.063	1.0575	0.4008	2.6385

*From [4].
†Single crystal specimen, see [4].

stability of the pyrochlore structure.* However, changes in the lattice distortion and/or lattice parameter might be anticipated. To study the phase stability and lattice distortion, we varied the charge on the B site by changing the number of B′ and B″ ions. A combination of Zn(B′) and Nb(B″) was chosen because Pb(Zn, Nb)O composition forms pyrochlore as the only stable phase in ceramic samples prepared by normal powder processing methods [4].† The general formula is written as $Pb(Zn_xNb_{1-x})O_{3.5-1.5x}$.

2. Experimental procedures

The nominal compositions of the compounds prepared are such that their chemical formulae should assume the form of $Pb(Zn_xNb_{1-x})O_{3.5-1.5x}$. The compositions studied, the corresponding B-site charge and oxygen concentration are listed in Table II.

High purity Nb_2O_5 (99.9% from Atomergic Chemicals Corp., Plainview, New York, USA) was used. Lead oxide and zinc oxide were of reagent grade (from Fisher Scientific, Fairlawn, New Jersey, USA). The oxides were mixed on the basis of 1 mole of PbO and ball-milled for 16 h in de-ionized water contained in a 16 oz (533 ml) polyethylene bottle using 1000 g ZrO_2 milling media. The mixtures were then filtered, dried and granulated. Each mixture was calcined in air at 800° C for 4 h in covered platinum crucibles. Subsequently, the powder was ball-milled for another 4 h to remove agglomeration. From these powders, approximately 10 g lots were heated in air at selected temperatures between 800 and 1300° C to determine the melting temperature and lattice parameter. The products at selected temperatures were examined by powder X-ray diffraction. A Phillips Model 3100 automated powder XRD unit was used with copper radiation filtered through nickel. Identification of phases was based on diffraction peaks in the 2θ range of 20° to 80°. Unit cell lattice constants were obtained using the (666) peak of the pyrochlore phase, at a scanning rate of 0.01° per step and a counting rate of 1 sec per step.

TABLE II Some characteristics of the pyrochlore compounds $Pb(Zn_xNb_{1-x})O_{3.5-1.5x}$.

x	+charge on B-site	Number of oxygen	Melting temperature (° C)	Lattice parameter (nm)
0	5.0	3.50	1270	1.0622 (α = 89.7°)
0.1	4.7	3.35	1295	1.0609 ± 0.0001
0.2	4.4	3.20	1220	1.0604 ± 0.0003
0.3	4.1	3.05	1205	1.0607 ± 0.0001
0.33	4.0	3.00	1200	1.0611 ± 0.0002
0.4	3.8	2.90	1190	1.0609

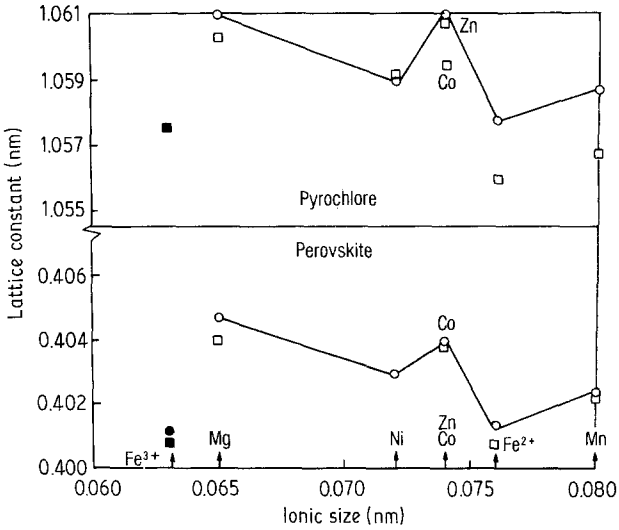

Figure 1 Lattice constants of the perovskite and pyrochlore phase as a function of the ionic size of the divalent cation [4]. (○ Nb^{5+}, □ Ta^{5+})

To measure the dielectric properties, approximately 0.5 g of the calcined powder was pressed into 0.65 cm diameter disc under 6.9×10^7 Pa (10 000 psi) and sintered in oxygen for 2 h at various temperatures. Electrical contacts were made by ultrasonically applying indium electrodes on the two flat surfaces of the discs. The dielectric constant and dissipation factor (tan δ) were then measured using HP4270A and HP4275A LCR meters (from Hewlett Packard, Palo Alto, California 94303, USA) at frequencies between 1 kHz and 10 MHz. Temperature dependence was obtained using a controlled-temperature chamber (Ransco Model 924) in conjunction with the LCR meters.

3. Results and discussion

3.1. Identification of phases

In all the compositions examined, the pyrochlore phase has formed at a calcination temperature of 800° C. Occasionally there are some very weak, extraneous diffraction peaks with intensity less than 1% of the strongest peak. At higher calcination temperatures, the diffraction peaks generally become sharper and there are less of the extraneous peaks.

At the nominal composition $Pb_2Nb_2O_7$ (x = 0), the X-ray pattern matches closely with that given in the X-ray powder diffraction data file‡. This is shown in

*If the formula is written as $Pb_2B_xO_y$, the number of oxygen can vary between 6 and 7.
†With suitable fluxes, single crystals of perovskite $Pb(Z_{1/3}Nb_{2/3})O_3$ can be grown.
‡JCPDS Diffraction File 25-444.

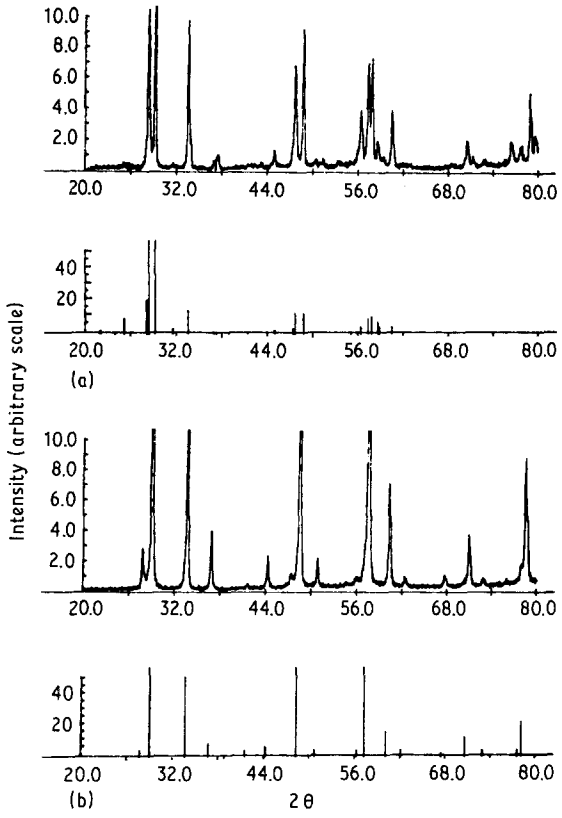

Figure 2 X-ray diffraction patterns of $Pb(Zn_xNb_{1-x})O_{3.5-1.5x}$ compositions (a) $x = 0$ calcined at 1250° C and (b) $x = 0.1$ calcined at 800° C.

Fig. 2a for powder calcined at 1250° C for 1/2 hr. The intensity scales for both the X-ray pattern and the reference file, were expanded for a better comparison of the weaker peaks. While this card file describes the crystal structure as monoclinic, earlier work by Cook and Jaffe [2], Goodman [5] and Jona *et al.* [3], all characterized the structure as rhombohedral. Assuming a rhombohedral lattice, the lattice parameters were calculated from the (666) and ($66\bar{6}$) diffraction lines yielding $a = 1.06224$ nm and $\alpha = 89°43'$. These values are somewhat different from the constants reported by the previous authors.*

As zinc was used to replace some of the niobium, the X-ray pattern changes to that of the cubic pyrochlore structure. Both the *d*-spacings and the relative intensity of the diffraction peaks correspond closely to the pattern of $Nd_2Zr_2O_7$.† This is shown in Fig. 2b for the $x = 0.1$ composition calcined at 800° C for 4 h, and the XRD intensity scale was also expanded for the purpose of comparison. Because there are no extra diffraction peaks, the zinc and niobium ions must occupy the B-site randomly. Contrary to the claim of Swartz and Shrout [6] the cubic pyrochlore that we observed does not match the X-ray pattern of $Pb_3Nb_4O_{13}$.‡

It is apparent that the rhombohedral lattice is limited to a narrow range near pure $Pb_2Nb_2O_7$. This is not only true for substitution in the B-site. Jona *et al.* [3] studied the A-site substitution in the system

TABLE III X-ray diffraction peaks observed in compositions $Pb(Zn_xNb_{1-x})O_{3.5-1.5x}$ calcined at 800° C for 4 h

2θ (deg)	*d* spacing (nm)	Relative integrated intensity	
		$x = 0.1$	$x = 0.33$
27.84	0.320 48	6.6	6.2
28.60	0.312 15	0	13.3
29.05	0.307 37	100.0	100.0
31.73	0.282 04	0	5.1
33.66	0.266 31	36.8	36.2
34.37	0.260 91	0	2
35.67	0.251 75	0	2.6
36.20	0.248 12	0	4.4
36.85	0.243 90	10.0	8.8
44.25	0.204 69	5.0	4.4
45.61	0.198 90	0	1.1
47.44	0.191 65	2.4	3.2
48.48	0.187 79	58.6	58.1
50.88	0.179 48	4.3	3.8
54.68	0.167 87	0.5	3.5
55.99	0.164 25	1.4	1.6
56.58	0.162 66	0	3.3
57.49	0.160 30	60.8	56.7
60.29	0.153 50	18.2	17.8
62.33	0.148 97	1.4	1.4
62.86	0.147 85	0	2.0
67.82	0.138 19	1.7	2.4
70.92	0.132 88	7.4	7.4
72.85	0.129 84	1.0	1.0
78.55	0.121 78	22.0	19.1

$(Cd_xPb_{1-x})_2Nb_2O_7$ and concluded that the phase boundary between the rhombohedral and cubic structures lies somewhere between $x = 0.1$ and $x = 0$. In this connection, it is of interest to note that Cook and Jaffe [2] reported a cubic lead niobate with the composition $Pb_{1.5}Nb_2O_{6.5}$. Thus, substitution in either the A or B-site by a small amount (< 0.1 lattice site) of cations with different valencies and/or ionic sizes alters the crystal structure from the rhombohedral $Pb_2Nb_2O_7$.

As the zinc concentration is increased above $x = 0.1$, there is a small change in the room temperature X-ray diffraction pattern. Fig. 3 shows this change in the 2θ range from 25° to 65°. While the X-ray patterns basically still match the cubic pyrochlore structure represented by $Nd_2Zr_2O_7$† several new but very weak peaks come into existence at various zinc concentrations. These peaks are marked by arrows and numbered in Fig. 3 at the concentration where each first appears. For some, the relative intensity changes with the concentration x, such as peaks 1 and 6. In Table III, we compare all the X-ray peaks that are observed in the compositions $x = 0.1$ and $x = 0.33$. The relative intensities of most peaks do not change significantly. However, there are eight extra peaks in the composition of $x = 0.33$. We shall assume that the pyrochlore phase remains cubic and that deficiency in oxygen ions with increasing x changes the extinction rule, leading to the appearance of the weak diffraction peaks. Remarkably, the composition with $x = 0.4$ shows the same diffraction pattern as $x = 0.33$. This suggests that it may still

*Cook and Jaffe: $a = 1.0570$ nm, $\alpha = 89° 15'$; Goodman: $a = 1.064$ nm, $\alpha = 88° 50'$; Jona, *et al.* $a = 1.0674$ nm, $\alpha = 88° 50'$.
†JCPDS Diffraction File 17-458. In the 2θ range scanned, only a very weak diffraction line at 47.44° cannot be identified.
‡JCPDS Diffraction File 25-443.

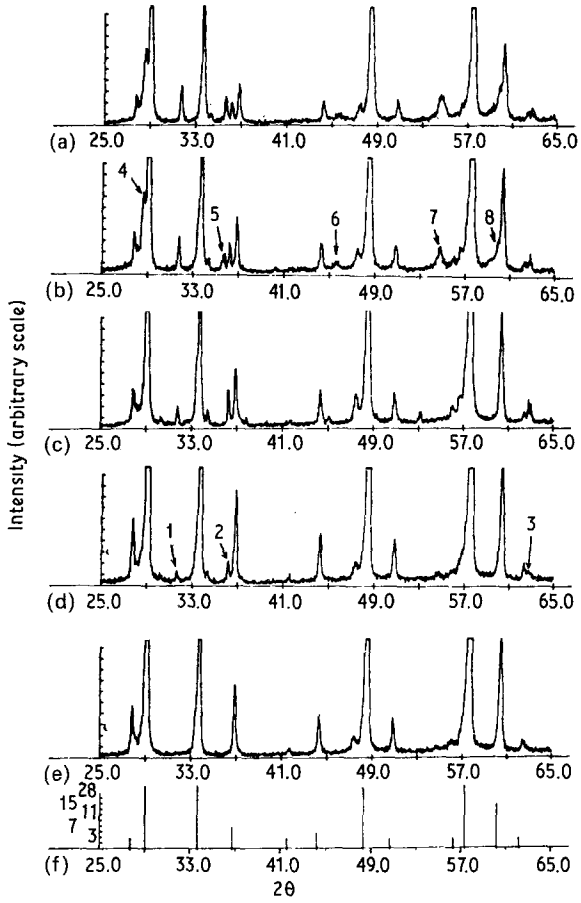

Figure 3 X-ray diffraction patterns of $Pb(Zn_xNb_{1-x})O_{3.5-1.5x}$ compositions calcined at 800° C. (a) $x = 0.4$, (b) $x = 0.33$, (c) $x = 0.3$, (d) $x = 0.2$, (e) $x = 0.1$, (f) $Nd_2Zr_2O_7$.

maintain the same pyrochlore crystal structure, though Table II shows that the number (2.9) of oxygen ions is less than the number of 3.0 required for the stability of the oxygen octahedron.

In addition to the appearance of new diffraction peaks, the lattice parameter also varies with the zinc concentration, as shown in Fig. 4. At each composition, the scatter in the data represents a variation between different samples while the error bar indicates the possible variation in an individual X-ray scan. At the stoichiometric composition of $Pb_2Nb_2O_7$, $x = 0$, the structure is rhombohedral with $a = 1.06224$ nm and $\alpha = 89° 43'$. The lattice parameter of the cubic pyrochlore decreases to 1.0609 nm at $x = 0.1$, and to a minimum of 1.0604 ± 0.0003 nm at $x = 0.2$; then it increases to 1.0607 nm at $x = 0.3$ and to 1.0611 nm at $x = 0.33$. Qualitatively, one might reason that as the oxygen number decreases initially with increasing zinc concentration, there are more oxygen vacancies at the seventh oxygen site, resulting in a smaller oxygen–oxygen repulsion. Consequently, the lattice contracts slightly to give a smaller lattice parameter. However, the repulsion between the positive lead ions will prevent the unit cell from contracting significantly. On the contrary, the Pb–Pb repulsion will gradually become stronger without the moderating influence of the negative oxygen ions in the seventh sites. Thus, we observed a slight increase in the lattice parameter when the zinc concentration exceeds 0.2, or when the oxygen number drops below 3.20 (Table II). This concentration represents a vacancy of 60% in the seventh oxygen site.

At a concentration of $x = 0.33$, all the oxygen seventh sites are vacant and the lattice parameter apparently reaches a maximum value. Further increase in x should result in oxygen vacancies in the octahedral sites. However, the X-ray diffraction pattern of $x = 0.4$ is identical to that of $x = 0.33$ (Fig. 3), suggesting that a similar crystal structure is maintained at $x = 0.4$. The lattice parameter appears to remain unchanged, from 1.0611 nm at $x = 0.33$ to 1.0609 nm at $x = 0.4$.

3.2. Melting temperature

The melting temperatures, T_m, of the pyrochlore compounds were determined by heating a small amount of powder at temperature increments of 10°. Thus the accuracy is $\pm 5°$. The results are listed in Table II and plotted in Fig. 5. There is an increase in T_m from 1270° C at $x = 0$ to 1295° C at $x = 0.1$, followed by a monotonic decrease as the zinc concentration increases above $x = 0.1$. The melting temperatures are 1220° C at $x = 0.2$, 1205° C at $x = 0.3$ and 1190° C at $x = 0.4$.

There seems to be a correlation between changes in the melting temperature and the crystal structure. The melting point increases between $x = 0$ and 0.1, when

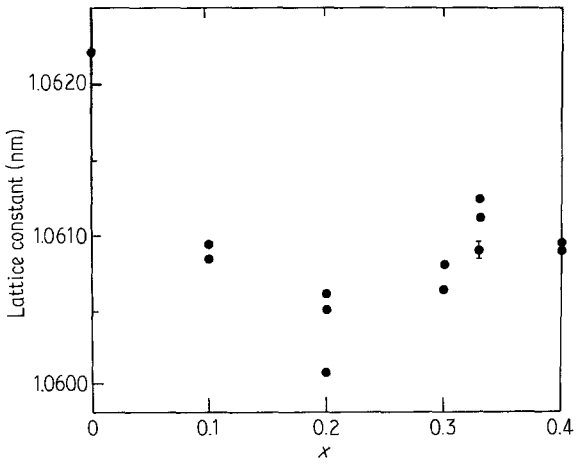

Figure 4 Variation of the lattice constant with the zinc concentration, x, in the $Pb(Zn_xNb_{1-x})O_{3.5-1.5x}$ compositions (calcined at 1100° C for 2 h static air).

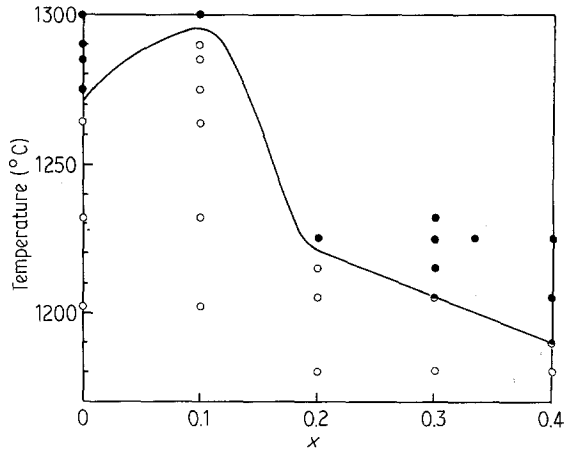

Figure 5 Phase-temperature diagram in the $Pb(Zn_xNb_{1-x})O_{3.5-1.5x}$ system. (● melted, (◓) partially melted, ○ solid)

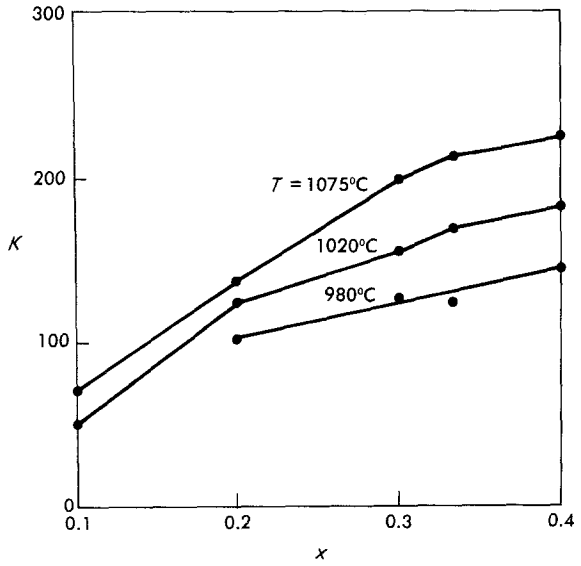

Figure 6 Variation of the dielectric constant, K, as a function of zinc concentration, x, at the sintering temperatures of 980, 1020 and 1075° C.

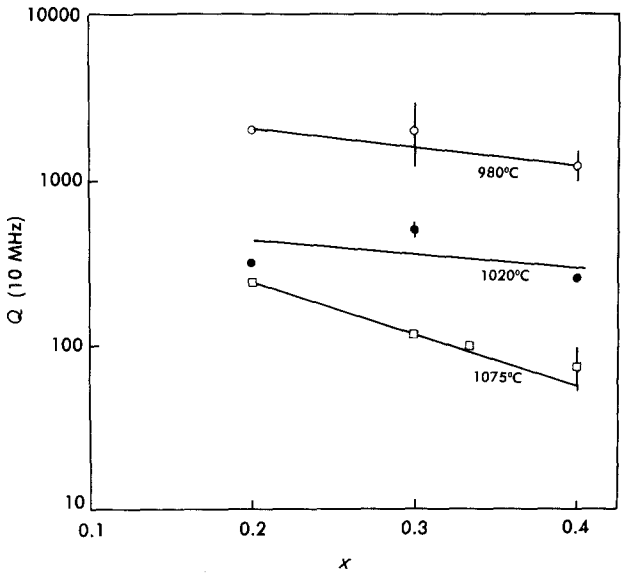

Figure 8 The Q factor at 10 MHz plotted against the zinc concentration, x, at the sintering temperatures of 980, 1020 and 1075° C.

the structure changes from rhombohedral to cubic pyrochlore. Between $x = 0.1$ and $x = 0.2$, a sharp decrease in T_m is accompanied by the appearance of new and weak diffraction peaks. A further decrease in T_m between $x = 0.2$ and 0.4 corresponds to additional changes in the X-ray diffraction pattern. These variations in T_m reflect the change in the crystal cohesive energy, which is a function of the various bond energies. The latter energies obviously depend on the crystal structure and environment, such as the zinc concentration or oxygen vacancies.

3.3. Dielectric properties

Samples with the compositions of $x = 0$ and 0.1 did not sinter to dense pellets at temperatures between 980 and 1075° C. Very often they cracked during the process of applying electrodes. Fig. 6 shows the dielectric constant measured at 1 kHz and at room temperature as a function of the composition. Data at three sintering temperatures are shown. The dielectric constant, K, increases monotonically with increasing zinc concentration and sintering temperature, with a maximum value of 225 at $x = 0.4$. The same K values are plotted differently in Fig. 7 as a function of sintering temperature. When measured between 1 kHz and 10 MHz, variation in the dielectric constant is less than 5% for all the compositions.

The Q factor, which is defined as $1/\tan \delta$, behaves in a manner opposite to the dielectric constant. Fig. 8 shows the Q factor at 10 MHz plotted against the composition for the same three sintering temperatures. Q decreases with increasing zinc concentration and with increasing sintering temperature. A maximum Q of 2000 is attained at 980° C.

Thus, we have to optimize two variables, composition and sintering temperature, in order to arrive at a high Q dielectric material with a reasonably high K value. If the major criterion is $Q > 1000$ at 10 MHz, the logical solution is to pick a composition of $Pb(Zn_xNb_{1-x})O_{3.5-1.5x}$ with $0.3 \leqslant x \leqslant 0.4$ and a sintering temperature of 980° C. The variation of Q with frequency is shown in Fig. 9 for two

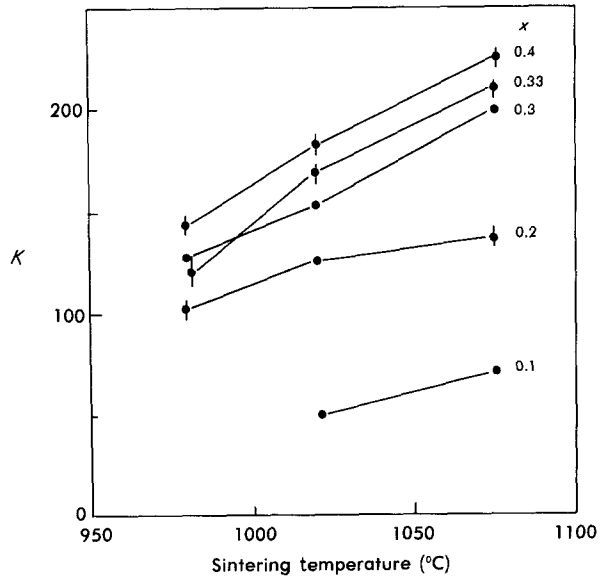

Figure 7 Variation of the dielectric constant, K, as a function of the sintering temperature for different zinc concentrations, x.

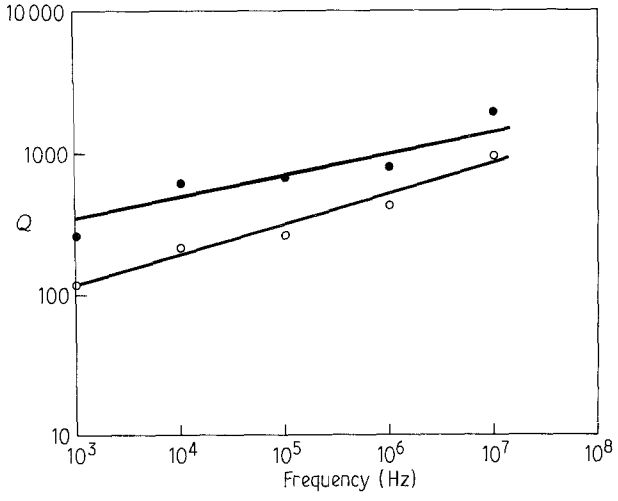

Figure 9 Variation of the Q factor with measuring frequency for $x = 0.3$ (●, $K = 124$) and 0.4 (○, $K = 136$) compositions sintered at 980° C for 2 h.

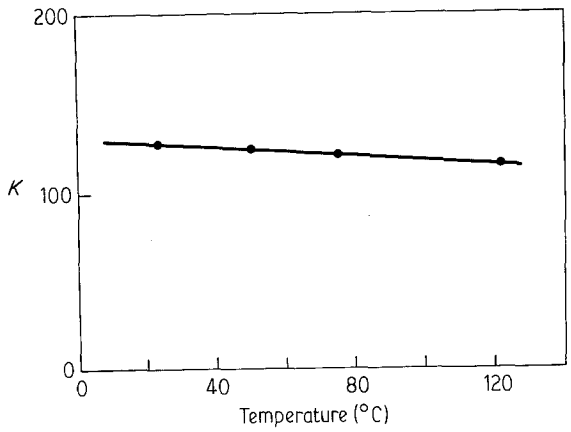

Figure 10 Temperature dependence of the dielectric constant at 1 kHz for the $x = 0.3$ composition sintered at 980° C for 2 h. TC = -0.75×10^{-3}° C^{-1}.

compositions, $x = 0.3$ and 0.4. Between 10^3 and 10^7 Hz, log Q increases linearly with log frequency, and the slopes for both compositions are quite similar.

The temperature dependence of the dielectric constant is shown in Fig. 10 for the $Pb(Zn_{0.3}Nb_{0.7})O_3$ composition. It shows a temperature coefficient of -0.75×10^{-3}° C^{-1} between 0 and 125° C. For the other compositions, the temperature coefficients are -0.75×10^{-3}° C^{-1} for both $x = 0.2$ and 0.33 and -0.55×10^{-3}° C^{-1} for $x = 0.4$.

3.4. $(1 - y)Pb(Zn_{1/3}Nb_{2/3})O_3 + yPbTiO_3$ compositions

In order to improve the temperature coefficient of a low K dielectric, it is customary to add a non-interacting second phase with a compensating temperature coefficient. Utilizing the logarithmic rule of mixing [7], the dielectric constant of the mixture is given by

$$\ln K = V_1 \ln K_1 + V_2 \ln K_2 \quad (1)$$

and the temperature coefficient by

$$\frac{1}{K}\frac{dK}{dT} = V_1\left(\frac{1}{K_1}\frac{dK_1}{dT}\right) + V_2\left(\frac{1}{K_2}\frac{dK_2}{dT}\right) \quad (2)$$

or

$$\tau = V_1\tau_1 + V_2\tau_2 \quad (3)$$

where V_1 and V_2 are the volume fractions of the two phases, and τ_1 and τ_2 are their temperature coefficients respectively.

In an attempt to improve the temperature coefficient of the $Pb(Zn_xNb_{1-x})O_{3.5-1.5x}$ pyrochlore compositions, we added varying amounts of $PbTiO_3$, which has a Curie temperature at 490° C. Because T_c is far above room temperature, $PbTiO_3$ has a small positive temperature coefficient (2×10^{-3}° C^{-1}) near room temperature for the dielectric constant. Then it may be possible to reduce the temperature coefficient of the resultant mixture.

$PbTiO_3$ was added in the amounts of 2, 5 and 10 mol % to $Pb(Zn_{1/3}Nb_{2/3})O_3$ pyrochlore. The mixture was ball-milled for 3 h in a plastic jar using ZrO_2 milling media. After filtering and drying, the mixture was granulated through a 20 mesh screen. Discs were pressed under 10 000 psi and sintered in oxygen. The phase composition was first analysed using X-ray diffraction. Both perovskite and pyrochlore peaks were observed in all three compositions, with the perovskite diffraction intensities increasing rapidly as more $PbTiO_3$ was added. Table IV lists the intensity ratio for samples sintered at 1050° C for 2 h. There is a dramatic increase in the volume fraction of the perovskite phase as the mole fraction of $PbTiO_3$ in the starting powder was increased from 0.05 to 0.10. Furthermore, the perovskite phase has cubic symmetry, with a lattice parameter of 0.405 ± 0.001 nm. This is different from the tetragonal symmetry that $PbTiO_3$ would have assumed at room temperature ($a = 0.3899$ nm, $c = 0.41532$ nm). And the measured lattice parameter of 0.405 nm is very close to the value of 0.404 nm obtained for the $Pb(Zn_{1/3}Nb_{2/3})O_3$ perovskite. Thus, one is led to suspect that at least some of the $Pb(Zn_{1/3}Nb_{2/3})O_3$ pyrochlore phase in the starting mixture has transformed into the $Pb(Zn_{1/3}Nb_{2/3})O_3$ perovskite phase, the transformation being facilitated by the presence of titanium ions. It is also likely that the perovskite phase incorporates titanium in the B sites, forming a compound of the form $Pb[(Zn_{1/3}Nb_{2/3})_\delta Ti_{1-\delta}]O_3$. More work is needed to identify the cause of the transformation. Furthermore, because of this reaction between $PbTiO_3$ and $Pb(Zn_{1/3}Nb_{2/3})O_3$ pyrochlore, the dielectric constants and the temperature coefficients of the constituent phases are not preserved in the reacted sample. Thus the logarithmic rule of mixing no longer applies.

The temperature dependence of the dielectric constant of the three compositions is shown in Fig. 11 for samples sintered at 980° C for 2 h in oxygen. The $y = 0.02$ composition exhibits a slightly smaller negative temperature dependence than the $Pb(Zn_{1/3}Nb_{2/3})O_3$ compositions, with temperature coefficient, TC = -0.66×10^{-3}° C^{-1} between 0 and 125° C. When the $PbTiO_3$ content is increased to 0.05, the negative TC becomes smaller and equals -0.54×10^{-3}° C^{-1} between 0 and 125° C. A positive temperature dependence begins to set in at temperatures above 140° C. The dielectric constant is also larger than the $y = 0.02$ composition. At a higher concentration of $PbTiO_3$, e.g. $y = 0.10$, the dielectric constant increases monotonically with temperature between −60 and 160° C at an average rate of 2.9×10^{-3}° C^{-1}. The K value is also much larger, between 400–1000 for $y = 0.10$ as compared to K of 120–150 for the $y = 0.02$ and 0.05 compositions.

Changes in the dissipation factor ($\tan \delta = 1/Q$) with temperature are shown in Fig. 12. Data at measuring frequencies of 1 kHz and 1 MHz are presented. In general, $\tan \delta$ increases with the concentration of $PbTiO_3$. For the $y = 0.02$ composition,

TABLE IV Relative X-ray diffraction intensities in compositions $yPbTiO_3 + (1 - y)Pb(Zn_{1/3}Nb_{2/3})O_3$ sintered at 1050° C

y	$I_{pero}^{(110)}$	$I_{pyro}^{(222)}$	$I_{pero}^{(110)}/[I_{pero}^{(110)} + I_{pyro}^{(222)}]$
0.02	1.76	100	0.017
0.05	8.61	100	0.079
0.10	100	81	0.553

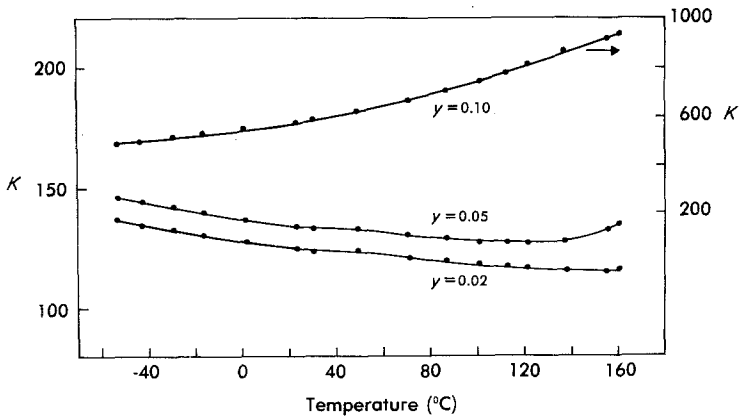

Figure 11 Temperature dependence of the dielectric constant in the $(1 - y)Pb(Zn_{1/3}Nb_{2/3})O_3 + yPbTiO_3$ compositions sintered at 980° C for 2 h.

tan δ is smaller than 0.004 at frequencies between 10^3 and 10^6 Hz and in the temperature range of -55 to 80° C. At higher temperature, tan δ at 1 kHz starts to increase, reaching a value of 0.02 at 140° C while at 1 MHz, tan δ remains constant at 0.002. The $y = 0.05$ compositions follows the same trend, with a slightly higher 1 kHz tan δ value of 0.006 between -55 and 90° C and then increases to 0.03 at 140° C. The 1 MHz tan δ actually decreases from 0.005 at 0° C to 0.002 at 140° C. The $y = 0.10$ composition has a larger tan δ, which is between 0.015 and 0.012 at 1 kHz and between 0.024 and 0.016 at 1 MHz in the temperature range of interest.

4. Conclusions

In lead-based ceramics with nominal compositions $Pb(B'_xB''_{1-x})O_3$ where the B site has an average charge of 4+, it is customary to find a mixture of cubic pyrochlore and perovskite phases after calcination. Based on X-ray diffraction analysis, we concluded that both phases are made up of the same structural unit of BO_6 octahedra. The B′ and B″ ions occupy the B sites randomly to the extent that local charge equilibrium is maintained. In the pyrochlore structure, the BO_6 octahedra share corners, with the two lead cations and an additional seventh oxygen site occupying the open space in the network. However, the seventh oxygen ion is not needed for the stability of the octahedra framework. Thus the general formula of the pyrochlore phase can be expressed as $Pb(B'_xB''_{1-x})O_3 \cdot O_p$ where $O \leqslant p \leqslant 0.5$.

In the $Pb(Zn_xNb_{1-x})O_{3.5-1.5x}$ system, where $p = 0.5\text{–}1.5x$, varying the zinc concentration x causes changes in the lattice constant as well as several new but weak X-ray diffraction lines to appear. We interpret this evidence as indicative of the changing occupancy of the seventh oxygen sites in order to maintain local charge balance. At $x = 1/3$, all the seventh oxygen sites are not occupied.

In order to arrive at the desirable dielectric properties of high Q and a reasonably high K value, we have to optimize two variables: composition and sintering temperature. A composition of $Pb(Zn_xNb_{1-x})O_{3.5-1.5x}$ with $0.3 \leqslant x \leqslant 0.4$ and a sintering temperature of 980° C give the best combination, with $125 \leqslant K \leqslant 135$ and $Q > 1000$ at 10 MHz. The temperature coefficient of the dielectric constant varies between -0.75 to $-0.55 \times 10^{-3}\,°C^{-1}$ for all the compositions studied.

By adding 2 mol % of $PbTiO_3$, which has a perovskite structure and a positive temperature coefficient, to the $Pb(Zn_{1/3}Nb_{2/3})O_3$ pyrochlore, the temperature coefficient is decreased from $-0.75 \times 10^{-3}\,°C^{-1}$ to $-0.66 \times 10^{-3}\,°C^{-1}$ between 0 and 125° C. At 5 mol % $PbTiO_3$ addition, the temperature coefficient decreases to $-0.54 \times 10^{-3}\,°C^{-1}$. Both the dielectric constant and Q do not change significantly. Thus, it may be possible to effect a larger change in the temperature coefficient by judiciously including selective amounts of a second phase which has the best compensating temperature coefficient.

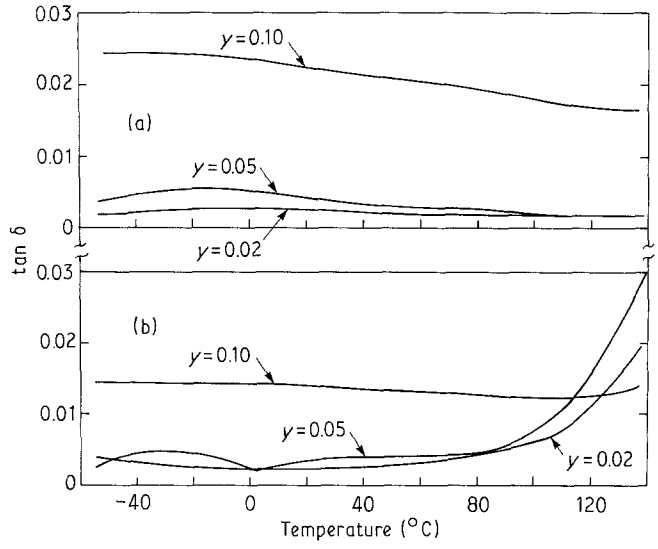

Figure 12 Temperature dependence of tan δ $(= 1/Q)$ in the $(1 - y)Pb(Zn_{1/3}Nb_{2/3})O_3 + yPbTiO_3$ compositions sintered at 980° C for 2 h in oxygen. (a) 1 MHz (b) 1 kHz.

References

1. A. BYSTROEM and A. KEMI, *Mineral. Geol.* **18A** (1944).
2. W. R. COOK, JR and H. JAFFE, *Phys. Rev.* **88** (1952) 1426.
3. F. JONA, G. SHIRANE and R. PEPINSKI, *Phys. Rev.* **98** (1955) 903.
4. H. C. LING, M. F. YAN and W. W. RHODES, to be published.
5. G. GOODMAN, *J. Amer. Ceram. Soc.* **36** (1953) 368.
6. S. L. SWARTZ and T. R. SHROUT, *Mater. Res. Bull.* **17** (1982) 1245.
7. A. E. PALADINO, *J. Amer. Ceram. Soc.* **54** (1971) 168.

Received 25 January
and accepted 10 June 1988